



## Free-volume defects investigation of GeS<sub>2</sub>-Ga<sub>2</sub>S<sub>3</sub>-CsI chalcogenide glasses by positron annihilation spectroscopy



Junpeng Li<sup>a,b</sup>, Guoxiang Wang<sup>a,b</sup>, Changgui Lin<sup>a,b</sup>, Tengyu Zhang<sup>a,b</sup>, Rui Zhang<sup>a,b</sup>, Zhaohuang Huang<sup>a,b</sup>, Xiang Shen<sup>a,b</sup>, Bingchuan Gu<sup>c,d</sup>, Bangjiao Ye<sup>c,d</sup>, Feifei Ying<sup>e</sup>, Maozhong Li<sup>e</sup>, Qihua Nie<sup>a,b,\*</sup>

<sup>a</sup>Laboratory of Infrared Materials and Devices, The Research Institute of Advanced Technologies, Ningbo University, Ningbo 315211, China

<sup>b</sup>Key Laboratory of Photoelectric Detection Materials and Devices of Zhejiang Province, Ningbo University, Ningbo 315211, China

<sup>c</sup>Department of Modern Physics, University of Science and Technology of China, Hefei 230026, China

<sup>d</sup>State Key Laboratory of Particle Detection and Electronics, University of Science and Technology of China, Hefei 230026, China

<sup>e</sup>North Yunnan Chihong photoelectric Co Ltd, Kunming 650000, China

### HIGHLIGHTS

- The free-volume defect of novel GeS<sub>2</sub>-Ga<sub>2</sub>S<sub>3</sub>-CsI glasses is investigated.
- The defects of the glasses were obviously reduced with increment of CsI.
- The atomic density  $\rho$  is inversely proportional to the number of these defects.

### ARTICLE INFO

#### Article history:

Received 17 December 2016

Revised 21 April 2017

Accepted 23 April 2017

Available online 24 April 2017

#### Keywords:

Chalcogenide glass  
Positron annihilation  
Free-volume defect  
Optical properties

### ABSTRACT

The transformation behavior of free-volume defect in (80GeS<sub>2</sub>-20Ga<sub>2</sub>S<sub>3</sub>)<sub>100-x</sub>(CsI)<sub>x</sub> ( $x = 0, 5, 10, 15$  mol%) chalcogenide glasses was studied by employing positron annihilation spectroscopic technique, which could reveal valuable information for in-depth understanding of nano-structural defects in glassy matrix. The results indicate that the structural changes caused by CsI additives can be adequately described by positron trapping modes determined with two-state model. The initial addition of CsI ( $x = 5$  mol%) led to a void contraction, whereas, the void agglomeration occurred with the increase of CsI and the free-volume defects of the glasses were obviously reduced. The atomic density  $\rho$  is inversely proportional to the number of these defects. Meanwhile, the UV cut-off edge shifts toward short-wavelength with increasing of CsI. This study provides the valuable information of defects evolution in GeS<sub>2</sub>-Ga<sub>2</sub>S<sub>3</sub>-CsI glasses.

© 2017 Elsevier B.V. All rights reserved.

### 1. Introduction

The sulfide-based chalcogenide glasses (ChGs) such as GeS<sub>2</sub>-Ga<sub>2</sub>S<sub>3</sub> glasses possess exceptional transparency and high nonlinearity, which have been widely used in multispectral imaging lenses, chemical and biological sensors, optical circuits, and planar waveguides [1–3]. However, disordered covalent-bonded networks proper to ChGs possess notable amount of free-volume defects formed due to the conventional melt-quenching technique [4]. The formation of free-volume defects influences the nonlinearity and optical stability of ChGs, which limiting the application in photonics further [5]. Therefore, the investigation on a free-

volume defects transformation in ChGs will be necessary to improve the performance of these materials. Numerous experimental techniques are employed to the investigation of the structure of these glasses, such as scanning electron microscopy (SEM), atomic force microscopy (AFM) and X-ray photoelectron spectroscopy (XPS), etc. Nevertheless, these experimental methods are limited to study the structure of atomic-deficient, especially in nanometer and sub-nanometer scale. Positron annihilation lifetime (PAL) spectroscopy is known as an informative tool for the investigation of free-volume defects in solids, which is grounded on physical phenomenon of electron interaction with its antiparticle (positron) in a matter [6,7]. In chalcogenide glasses, this method is used to identify intrinsic free volumes in the frame of the model that considers competitive channels-positron trapping in extended free-volume defects and positron electron (positronium) decaying in holes [6,8].

\* Corresponding author at: Key Laboratory of Photoelectric Detection Materials and Devices of Zhejiang Province, Ningbo University, Ningbo 315211, China.

E-mail address: [nieqihua1@126.com](mailto:nieqihua1@126.com) (Q. Nie).

Addition of alkali halides such as CsCl to GeS<sub>2</sub>-Ga<sub>2</sub>S<sub>3</sub> ternary system not only extends the transparency in the visible region but also influences the voids in the inner structure of the modified glassy matrix at the nanoscale [9]. In recent years, the free-volume defects of the GeS<sub>2</sub>-Ga<sub>2</sub>S<sub>3</sub>-CsCl glasses have been studied intensively [10], and it has been proved that the addition of CsCl could reduce the void defects. In view of the I and Cl located at the same group in chemical element periodic table, it maybe exhibits a similar physical and chemical properties. The transformation behavior of defects in CsI doped GeS<sub>2</sub>-Ga<sub>2</sub>S<sub>3</sub> glasses was investigated. In this paper, the GeS<sub>2</sub>-Ga<sub>2</sub>S<sub>3</sub>-CsI glasses were performed and the effect of CsI on structural defects in GeS<sub>2</sub>-Ga<sub>2</sub>S<sub>3</sub> glasses tested by positron annihilation technique has been investigated. The optical properties of the samples were also analyzed with X-ray diffraction, Raman scattering spectra and transmission spectral measurements. The study aims to provide the valuable information of the defects evolution with the CsI concentration in these glass samples.

## 2. Experimental

(80GeS<sub>2</sub>-20Ga<sub>2</sub>S<sub>3</sub>)<sub>100-x</sub>(CsI)<sub>x</sub> (x = 0, 5, 10, 15 mol%) glasses were prepared from Ge, Ga, S and CsI materials in silica ampoule kept under the vacuum of 10<sup>-3</sup> Pa. Materials were melted at 980 °C in a rocking furnace for 12 h. After that, the bulk samples were obtained by quenching in cold water. Finally, the GeS<sub>2</sub>-Ga<sub>2</sub>S<sub>3</sub>-CsI glasses were annealed at 10 °C below glass transition temperature T<sub>g</sub> to minimize inner strains. The obtain rods were cut into disks of ~1 mm and 2 mm in thickness and polished to a high optical quality.

The samples are examined by X-ray diffraction (XRD) apparatus with a power diffractometer (German Bruker D2) using Cu K<sub>α</sub> radiation (30 kV 20 mA) to confirm the amorphous states. Densities were measured according to Archimedes' principle with Density Determination Kit (ME-DNY-4, METTLER TOLEDO, Zürich, Switzerland) and the accuracy was ±0.001 g/cm<sup>3</sup>. The absorption spectra of samples were recorded in the range of 400–700 nm using Perkin-Elmer Lambda 950 UV-vis-NIR spectrophotometer. Raman spectroscopy was conducted at room temperature using the back (180°) scattering configuration by the Renishaw inVia Raman spectra with a LD laser with a wavelength of 785 nm. The resolution of the frequencies was ±1 cm<sup>-1</sup>. The PALS measurements were performed using a conventional fast-fast coincidence system with an ORTEC spectrometer of 230 ps resolution (FWHM of single Gaussian, determined by measuring <sup>60</sup>Co isotope) at the temperature T = 24 °C and relative humidity RH = 37%. In each measurement, the <sup>22</sup>Na radioactive source was placed between two identical polished samples like a typical sandwich geometry, used as a source of positrons. The contribution from a source was taken at a level of 8.9%. Each PAL spectrum was recorded in a high-measurement statistics of ~2 × 10<sup>6</sup> coincidences to ensure a precise lifetime measurement. The channel width of 6.37 ps allows the total number of channels up to 8000. The raw PAL spectra of the investigated glasses were processed with LT 9.0 program.

## 3. Results and discussions

Fig. 1 shows the X-ray diffraction patterns of the (80GeS<sub>2</sub>-20Ga<sub>2</sub>S<sub>3</sub>)<sub>100-x</sub>(CsI)<sub>x</sub> glass samples, where x = 0 (G0), 5 (G5), 10 (G10), 15 (G15), respectively. These glasses are yellow and nearly transparent in the visible region. In order to confirm the amorphous state of each sample, XRD analysis was conducted. According to Fig. 1, the amorphous state of the glasses was confirmed. The diffraction intensity has only some fluctuations with the instrumental background line when 2θ of the scanning range increases. It manifests that there are no sharp peaks and crystalline

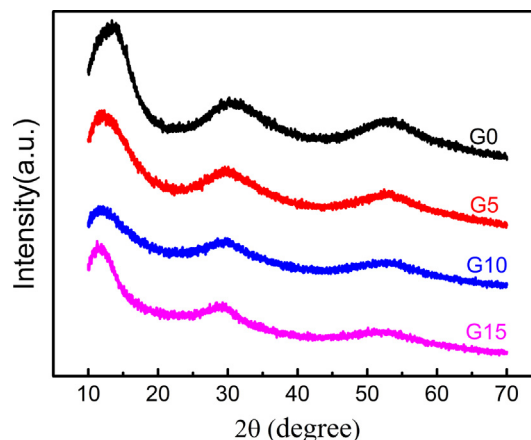


Fig. 1. XRD patterns of the (80GeS<sub>2</sub>-20Ga<sub>2</sub>S<sub>3</sub>)<sub>100-x</sub>(CsI)<sub>x</sub> (x = 0, 5, 10, 15 mol%) glass samples.

phases appeared, implying the typical amorphous nature [11], which is necessary for avoiding the crystalline state to bring errors to the positron annihilation test later.

Fig. 2 presents the vis-NIR absorption spectra of (80GeS<sub>2</sub>-20Ga<sub>2</sub>S<sub>3</sub>)<sub>100-x</sub>(CsI)<sub>x</sub> (x = 0, 5, 10, 15 mol%) glasses. The short-wavelength cut-off edge of the glasses with light yellow color locates at ~450 nm. It is obvious that the short-wavelength cut-off edge shifts toward a shorter wavelength with the increase of CsI content, which is determined by the electrical transition between valence bands and conduction bands [12]. The reason is that Cs<sup>+</sup> and I<sup>-</sup> atoms are of less polarizability compared with Ge<sup>2+</sup>, Ga<sup>3+</sup> and S<sup>2-</sup> [13] and the average electron affinity energy of I<sup>-</sup> is bigger than that of S<sup>2-</sup> [14]. Therefore, the required excitation energy of electronic transition is greater, resulting in the short-wavelength cut-off edge shorter [15].

To elucidate the structural evolution, Raman spectra were recorded and collected as shown in Fig. 3. Two main regions in these spectra are distinguishable: (a) there is a decreasing trend of dominate band at 340 cm<sup>-1</sup> along with shoulder around 370 and 430 cm<sup>-1</sup>, respectively, (b) with increasing of CsI content, the broad bands between 200 and 300 cm<sup>-1</sup> have an inverse change in intensity. According to the previous studies of Raman spectra in GeS<sub>2</sub>-Ga<sub>2</sub>S<sub>3</sub> based glasses, the most intense band at 340 cm<sup>-1</sup> is attributed to the overlap of (ν<sub>1</sub>) symmetric stretching modes of [Ge(Ga)S<sub>4</sub>] tetrahedral [16], while the shoulder at 370 cm<sup>-1</sup> corresponds to the edge-sharing [Ge(Ga)S<sub>4</sub>] units [17].

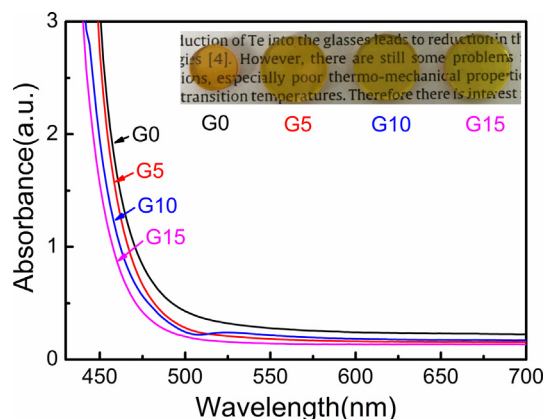


Fig. 2. The vis-NIR absorption spectra of (80GeS<sub>2</sub>-20Ga<sub>2</sub>S<sub>3</sub>)<sub>100-x</sub>(CsI)<sub>x</sub> (x = 0, 5, 10, 15 mol%) glass samples. The inset shows the picture of these glasses.

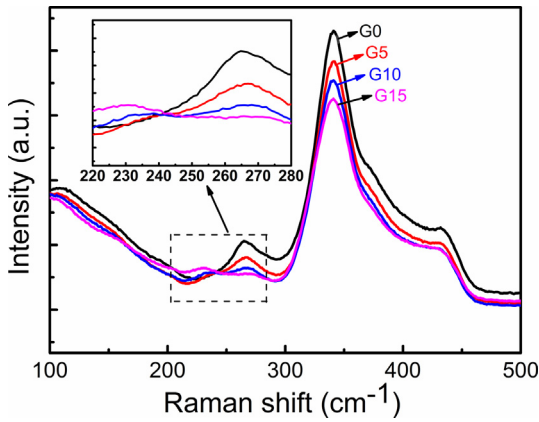


Fig. 3. Raman spectra of  $(80\text{GeS}_2-20\text{Ga}_2\text{S}_3)_{100-x}(\text{CsI})_x$  ( $x = 0, 5, 10, 15$  mol%) glass samples. The inset is an amplification ranging from  $220$  to  $280$   $\text{cm}^{-1}$ .

There is still a controversial problem now about the ascription of the band at  $430$   $\text{cm}^{-1}$ . The intensity decreases from  $340$  to  $370$   $\text{cm}^{-1}$  with the increasing CsI. It is due to the formation of  $[\text{Ge}(\text{Ga})\text{S}_3\text{I}]$  units. In the inset of Fig. 3, the variation of these Raman bands attracts more attention. This change can be split into two bands that are located near  $240$  and  $270$   $\text{cm}^{-1}$ , respectively. It is well known that the band at  $240$   $\text{cm}^{-1}$  is associated with the asymmetrical stretching vibration ( $\nu_2$ ) of Ge-I in the  $[\text{S}_2\text{GeI}_2]$  structural units [18]. And the band at  $270$   $\text{cm}^{-1}$  is chiefly assigned to the  $[\text{S}_3\text{Ge}(\text{Ga})-(\text{Ga})\text{GeS}_3]$  ethane-like units [19]. With the addition of CsI, I atoms can substitute some S atoms in  $[\text{GeS}_4]$  tetrahedral, which leads to an increase in  $240$   $\text{cm}^{-1}$  Raman band due to the formation of  $[\text{S}_2\text{GeI}_2]$ . Meanwhile, the linkage of  $[\text{S}_3\text{Ge}(\text{Ga})-(\text{Ga})\text{GeS}_3]$  ethane-like unit have been broken with lack of sulfur, leading to the formation of the mixed-anion  $[\text{I}_x\text{S}_{3-x}\text{Ge}(\text{Ga})-(\text{Ga})\text{GeS}_{3-x}\text{I}_x]$  unit. This will result in the decreasing feature of Raman band at  $270$   $\text{cm}^{-1}$ . Consequently, it is obvious that the connectivity of the glassy network is decreased with the break of Ge-S or Ga-S bonds in the  $\text{GeS}_2$ - $\text{Ga}_2\text{S}_3$ -CsI glasses. And the reduction of  $T_g$  also indicates that the glass network is loose with the addition of CsI [20]. The most possible explanation is that the free volume defects agglomeration with the increase of CsI results in the loosening network of glasses.

The typical PAL spectra of  $80\text{GeS}_2-20\text{Ga}_2\text{S}_3$  glasses are depicted in Fig. 4, which reconstructed from two-component fitting at general background of standard source contribution. It can be also decomposed into three combined positron-positronium components, but could not improve decomposition goodness signifi-

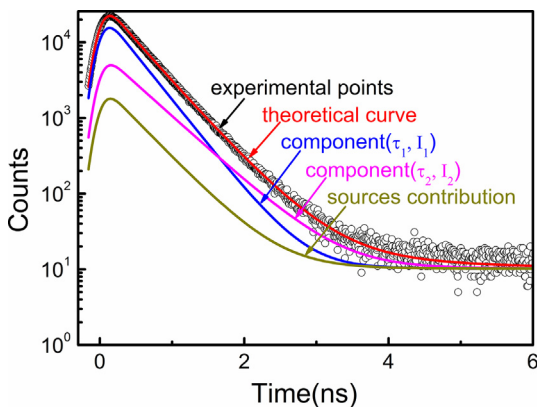


Fig. 4. Typical PAL spectrum for  $80\text{GeS}_2-20\text{Ga}_2\text{S}_3$  glass decomposed into two components.

cantly, the estimated input from this positronium component in the PAL spectra being less than 1% [21]. As a typical PAL spectrum of positron annihilation event histograms, this figure was characterized by narrow peaks and regions of long fluent decaying of coincidence counts in a time. According to Fig. 4, the contribution of standard sources is about 8.9%, which could be achieved satisfactorily within the permissible range of error. Thus, the decaying behavior of such curve can be represented by sum of two exponentials with the power inversely proportional to positron lifetimes  $\tau_1$  and  $\tau_2$  while the area under each of these exponential curves being proportional to the intensities  $I_1$  and  $I_2$  [22,23].

Fitting parameters for PAL spectra of  $(80\text{GeS}_2-20\text{Ga}_2\text{S}_3)_{100-x}(\text{CsI})_x$  ( $x = 0, 5, 10, 15$  mol%) glasses are given in Table 1, which is calculated with two-component fitting procedure. In H. Klym's works [24,25], it has been confirmed that the first component ( $\tau_1, I_1$ ) is of no physical meaning for chalcogenide glasses. The intensity  $I_2$  is proportional to the number of these voids, and the lifetime  $\tau_2$  shows the size of free voids where positrons are trapped [24–26]. Now, we will focus on analyzing the parameters of  $\tau_2$  and  $I_2$  which are regarded as the main nanostructural free-volume void transformation in  $\text{GeS}_2$ - $\text{Ga}_2\text{S}_3$ -CsI chalcogenide glasses with different amounts of CsI in the glass matrix. With the changes of CsI amount, the intensity  $I_2$  decreases and the lifetime  $\tau_2$  decreases first and then increases compared to  $80\text{GeS}_2-20\text{Ga}_2\text{S}_3$  glass. The addition of CsI results in voids contraction and agglomeration in glasses formation process as shown in Fig. 5.

The parameters of  $\tau_2$  and  $I_2$  for G5 are less than those of G0, indicating the voids contraction. In other words, the free-volume voids have shrunk accompanying with the reduction of defects in the number. With increasing of CsI content, the lifetime  $\tau_2$  of G10 increases slightly and the intensity  $I_2$  decreases, which means that the free-volume voids are expanded a little and some defects are vanished. In the case of G15, an obvious transformation is observed. The lifetime  $\tau_2$  increases from  $0.500$  ns for G10 glass to  $0.510$  ns for G15 glass and the intensity  $I_2$  decreases from  $0.263$  (a.u.) to  $0.230$  (a.u.). Such behavior corresponds to voids agglomeration, when the addition of CsI content is mainly responsible for the number of free-volume defects.

In order to investigate positron trapping rate and defects concentration, a quantitative analysis of positron trapping modes was taken by a so-called two-state positron trapping model [27–29]:

$$\tau_{av} = (\tau_1 I_1 + \tau_2 I_2) / (I_1 + I_2) \quad (1)$$

$$\tau_b = (I_1 + I_2) / (I_1 \tau_1^{-1} + I_2 \tau_2^{-1}) \quad (2)$$

$$\kappa_d = I_2 / I_1 (\tau_b^{-1} - \tau_d^{-1}) \quad (3)$$

where  $\tau_{av}$  is the average positron lifetime while  $\tau_b$  is the positron annihilation lifetime in bulk (defect-free region).  $\tau_d$  is equal to  $\tau_2$  which is the positron annihilation lifetime in defects, and  $\kappa_d$  is the total positron trapping rate at the defects. In addition, the difference ( $\tau_d - \tau_b$ ) demonstrates the size of expanded free-volume defects where positrons are trapped, and the ratio  $\tau_d/\tau_b$  was taken in a direct correlation to the nature of these defects [30].

The other positron trapping parameters are listed in Table 2, in order to comprehend the free-volume transformation more deeply. The average positron lifetime  $\tau_{av}$  and defect-free lifetime  $\tau_b$  almost have any changes with addition of CsI. The positron trapping rate  $\kappa_d$  in voids reduces mainly due to the drop of the intensity  $I_2$ . It is confirmed that the number of free-volume defects have reduced when the positron trapping rate in defects  $\kappa_d$  decreases with further CsI. From the previous Raman spectra, a plausible hypothesis is that the break of Ge-S or Ga-S bonds are associated with void

**Table 1**

Fitting parameters for PAL spectra of  $(80\text{GeS}_2-20\text{Ga}_2\text{S}_3)_{100-x}(\text{CsI})_x$  ( $x = 0, 5, 10, 15$  mol %) glasses.

Sample	$\tau_1$ (ns)	$I_1$ (a.u.)	$\tau_2$ (ns)	$I_2$ (a.u.)
G0	0.364	0.715	0.505	0.284
G5	0.365	0.728	0.499	0.272
G10	0.363	0.737	0.500	0.263
G15	0.365	0.770	0.510	0.230

transformations in glassy matrix [31]. Although the degree of glass network connectivity decreases, the samples possess a better optical property. Also, the contraction and agglomeration of free-volume voids in the inner structure of materials are described by other PAL parameters. The difference  $(\tau_2 - \tau_b)$  decreases from 0.109 ns to 0.104 ns, indicating that the free-volume voids have contracted due to unfavorable environment. However, with the further CsI, the  $\tau_2 - \tau_b$  increase from 0.104 ns to 0.119 ns, it is shown that the free volume void will expand by voids agglomeration.

Furthermore, the relationship between the positron trapping rate  $\kappa_d$  and density  $\rho$  have been studied as shown in Fig. 6. The positron trapping rate  $\kappa_d$  in defects decreases from  $0.217 \text{ ns}^{-1}$  to  $0.178 \text{ ns}^{-1}$ , while the density  $\rho$  increases with increasing of CsI content. There is an abnormal tendency in  $\kappa_d$ - $\rho$  correlation, and the free volume of positron trapping voids is mainly responsible for atomic density of the glasses [32]. In other words, it is possible

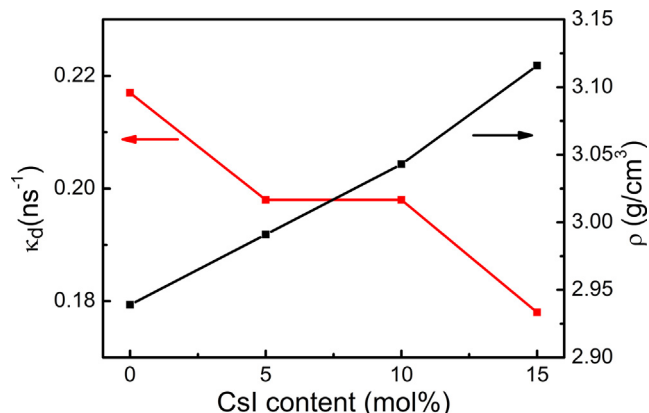


**Fig. 6.** The relationship between positron trapping rate  $\kappa_d$  and density  $\rho$  within different CsI content.

that the  $\text{Cs}^+$  occupied the position of defects, which can reduce the number of defects, meanwhile the atomic density of unit volume increased. This process is accompanied with void contraction and agglomeration.

The study also provides a chance to compare the void transformation between  $\text{GeS}_2\text{-Ga}_2\text{S}_3\text{-CsI}$  and  $\text{GeS}_2\text{-Ga}_2\text{S}_3\text{-CsCl}$  glassy matrices. According to the data from Table 1, Table 2 and Ref. [33], two major points can be concluded: (a) The changes of intensity  $I_2$  and

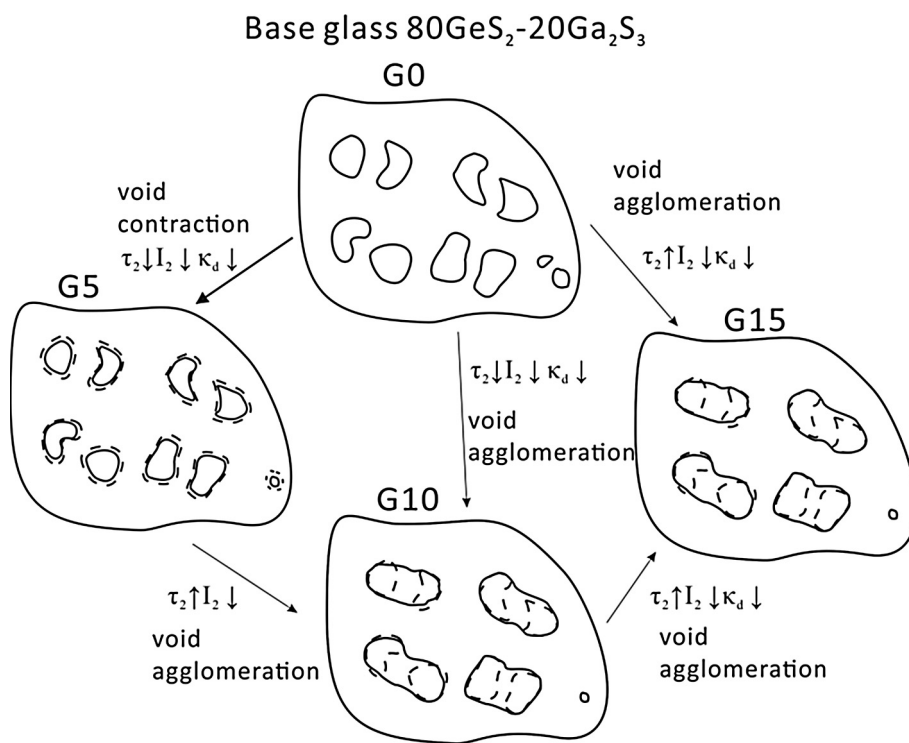


**Fig. 5.** Schematic assumption of nanoscale free-volume void evolution in  $\text{GeS}_2\text{-Ga}_2\text{S}_3\text{-CsI}$  chalcogenide glasses caused by CsI additions.

**Table 2**

Positron trapping modes for PAL spectra of  $(80\text{GeS}_2-20\text{Ga}_2\text{S}_3)_{100-x}(\text{CsI})_x$  ( $x = 0, 5, 10, 15$  mol %) glasses.

Sample	$\tau_{av}$ (ns)	$\tau_b$ (ns)	$\kappa_d$ ( $\text{ns}^{-1}$ )	$\tau_2 - \tau_b$ (ns)	$\tau_2 / \tau_b$
G0	0.404	0.396	0.217	0.109	1.27
G5	0.402	0.394	0.198	0.104	1.26
G10	0.399	0.399	0.198	0.108	1.27
G15	0.398	0.398	0.178	0.119	1.30

positron trapping rate  $\kappa_d$  in  $\text{GeS}_2\text{-Ga}_2\text{S}_3\text{-CsI}$  glasses have the same tendency with those in  $\text{GeS}_2\text{-Ga}_2\text{S}_3\text{-CsCl}$  glasses, indicating that the addition of halide can reduce the number of free-volume defects in  $\text{GeS}_2\text{-Ga}_2\text{S}_3$  glassy matrix. (b) The changes of lifetime  $\tau_2$  in both glass samples are different. In H. Klym's works [33], the lifetime  $\tau_2$  increases from 0.426 to 0.499 ns with the increase of CsCl concentration. This means that the size of the free-volume defects become larger by voids agglomeration in  $\text{GeS}_2\text{-Ga}_2\text{S}_3\text{-CsCl}$  glasses. In the case of  $(80\text{GeS}_2\text{-}20\text{Ga}_2\text{S}_3)_{85}(\text{CsCl})_{15}$  glass, the defects contract because of higher concentration of CsCl. In comparison, as for  $\text{GeS}_2\text{-Ga}_2\text{S}_3\text{-CsI}$  glasses, the lifetime  $\tau_2$  decreases from 0.505 ns to 0.499 ns with the increase of CsI content. The possible reason is that the initial CsI will bring the compactness of glass structure which results in a void contraction. With increasing of CsI content, the free-volume defects are expanded by voids agglomeration.

#### 4. Conclusion

In this study, a series of  $\text{GeS}_2\text{-Ga}_2\text{S}_3\text{-CsI}$  chalcogenide glasses were prepared by the conventional melt-quenching technique. The defects transformation behavior was systemically studied by positron annihilation measurement. For the glasses of  $(80\text{GeS}_2\text{-}20\text{Ga}_2\text{S}_3)_{100-x}(\text{CsI})_x$  ( $x = 0, 5, 10, 15 \text{ mol}\%$ ), the number of free-volume defects will be reduced with increasing of CsI content. The defects contraction was observed when CsI concentration is 5 mol%. With the further addition of CsI, the size of the defects become larger due to voids agglomeration. The atomic density  $\rho$  is inversely proportional to the number of these defects. The possible reason is that the  $\text{Cs}^+$  occupy the position of defects, resulting in the less number of defects and higher density of samples. The defects evolution with the CsI amount in these glass samples provides the valuable information of inner structure, which is useful for improving the quality of  $\text{GeS}_2\text{-Ga}_2\text{S}_3$  glasses or doping the rare earth ions.

#### Acknowledgments

This work was financially supported by the National Natural Science Foundation of China (Grant No. 61306147), the Open Foundation of State Key Laboratory of Infrared Physics (Grant No. M201510), the Natural Science Foundation of Zhejiang Province (Grant No. LQ15F040002), and was sponsored by the K. C. Wong Magna Fund and the Scientific Research Foundation of Graduate School at Ningbo University.

#### References

- [1] K. Abe, H. Takebe, K. Morinaga, Preparation and properties of Ge-Ga-S glasses for laser hosts, *J. Non-Cryst. Solids* 212 (1997) 143–150.
- [2] X.H. Zhang, Y. Guimond, Y. Bellec, Production of complex chalcogenide glass optics by molding for thermal imaging, *J. Non-Cryst. Solids* 326 (2003) 519–523.
- [3] L. Calvez, P. Lucas, M. Rozé, H.L. Ma, J. Lucas, X.H. Zhang, Influence of gallium and alkali halide addition on the optical and thermo-mechanical properties of  $\text{GeSe}_2\text{-Ga}_2\text{Se}_3$  glass, *Appl. Phys. A-Mater.* 89 (2007) 183–188.
- [4] A. Feltz, *Amorphous Inorganic Materials and Glasses*/Adalbert Feltz, VCH, 1993.
- [5] I.I. Kang, S. Smolorz, T. Krauss, F. Wise, B.G. Aitken, N.F. Borrelli, Time-domain observation of nuclear contributions to the optical nonlinearities of glasses, *Phys. Rev. B: Condens. Matter* 54 (1996) 12641–12644.
- [6] R. Krause-Rehberg, H.S. Leipner, *Positron Annihilation in Semiconductors: Defect Studies*, Springer, 1999.
- [7] G. Dlubek, Y. Yu, R. Krause-Rehberg, W. Beichel, S. Bulut, N. Pogodina, I. Krossing, C. Friedrich, Free volume in imidazolium triflimide ( $[\text{C}_3\text{MIM}][\text{NTf}_2]$ ) ionic liquid from positron lifetime: Amorphous, crystalline, and liquid states, *J. Chem. Phys.* 133 (2010) 124502.
- [8] Y.C. Jean, P.E. Mallon, D.M. Schrader, *Principles and Applications of Positron and Positronium Chemistry*, World Scientific, 2003.
- [9] H. Klym, A. Ingram, O. Shpotyuk, I. Karbovnyk, Influence of CsCl addition on the nanostructured voids and optical properties of  $80\text{GeS}_2\text{-}20\text{Ga}_2\text{S}_3$  glasses, *Opt. Mater.* 59 (2016) 39–42.
- [10] H. Klym, A. Ingram, O. Shpotyuk, Free-volume nanostructural transformation in crystallized  $\text{GeS}_2\text{-Ga}_2\text{S}_3\text{-CsCl}$  glasses, *Materialwiss. Werkst.* 47 (2016) 198–202.
- [11] G. Wang, Q. Nie, M. Barj, X. Wang, S. Dai, X. Shen, T. Xu, X. Zhang, Compositional dependence of the optical properties of novel Ge-Ga-Te-CsI far infrared transmitting chalcogenide glasses system, *J. Phys. Chem. Solids* 72 (2011) 5–9.
- [12] G. Dong, H. Tao, S. Chu, S. Wang, X. Zhao, Q. Gong, X. Xiao, C. Lin, Study on the structure dependent ultrafast third-order optical nonlinearity of  $\text{GeS}_2\text{-In}_2\text{S}_3$  chalcogenide glasses, *Opt. Commun.* 270 (2007) 373–378.
- [13] R.K. Pan, H.Z. Tao, C.G. Lin, H.C. Zang, X.J. Zhao, T.J. Zhang, On the optical properties of amorphous Ge-Ga-Se-KBr films prepared by pulsed laser deposition, *Appl. Surf. Sci.* 255 (2009) 5952–5956.
- [14] G. Tang, Z. Yang, L. Luo, W. Chen, Preparation and properties of  $\text{GeSe}_2\text{-Ga}_2\text{Se}_3\text{-KBr}$  new chalcogenide glasses, *J. Alloys Compd.* 459 (2008) 472–476.
- [15] M. De Sario, G. Leggeri, A. Luches, M. Martino, F. Prudeniano, A. Rizzo, Pulsed laser deposition of praseodymium-doped chalcogenide thin films, *Appl. Surf. Sci.* 186 (2002) 216–220.
- [16] C. Lin, L. Calvez, H. Tao, M. Allix, A. Moréac, X. Zhang, X. Zhao, Evidence of network demixing in  $\text{GeS}_2\text{-Ga}_2\text{S}_3$  chalcogenide glasses: A phase transformation study, *J. Solid State Chem.* 184 (2011) 584–588.
- [17] S. Sugai, Stochastic random network model in Ge and Si chalcogenide glasses, *Phys. Rev. B: Condens. Matter* 35 (1987) 478–479.
- [18] L. Koudelka, M. Pisárčik, Raman study of short-range order in  $\text{Ge}_x\text{S}_y\text{I}_z$  glasses, *J. Non-Cryst. Solids* 113 (1989) 239–245.
- [19] H. Guo, Y. Zhai, H. Tao, G. Dong, X. Zhao, Structure and properties of  $\text{GeS}_2\text{-Ga}_2\text{S}_3\text{-CdI}_2$  chalcogenide glasses, *Mater. Sci. Eng., B* 138 (2007) 235–240.
- [20] C. Lin, G. Qu, Z. Li, S. Dai, H. Ma, T. Xu, Q. Nie, X. Zhang, Correlation between crystallization behavior and network structure in  $\text{GeS}_2\text{-Ga}_2\text{S}_3\text{-CsI}$  chalcogenide glasses, *J. Am. Ceram. Soc.* 96 (2013) 1779–1782.
- [21] Y. Shpotyuk, A. Ingram, O. Shpotyuk, PAL spectroscopy of rare-earth doped Ga-Ge-Te/Se glasses, *J. Phys. Chem. Solids* 91 (2016) 76–79.
- [22] U. Brossmann, W. Puff, R. Würschum, *Positron Annihilation Studies of Materials*, 2003.
- [23] F. Tuomisto, I. Makkonen, Defect identification in semiconductors with positron annihilation: Experiment and theory, *Rev. Mod. Phys.* 85 (2013) 1583–1631.
- [24] O. Shpotyuk, L. Calvez, E. Petracovschi, H. Klym, A. Ingram, P. Demchenko, Thermally-induced crystallization behaviour of  $80\text{GeSe}_2\text{-}20\text{Ga}_2\text{Se}_3$  glass as probed by combined X-ray diffraction and PAL spectroscopy, *J. Alloys Compd.* 582 (2014) 323–327.
- [25] H. Klym, A. Ingram, O. Shpotyuk, L. Calvez, E. Petracovschi, B. Kulyk, R. Serkiz, R. Szatanik, 'Cold' crystallization in nanostructured  $80\text{GeSe}_2\text{-}20\text{Ga}_2\text{Se}_3$  glass, *Nanoscale Res. Lett.* 10 (2015) 49.
- [26] R. Golovchak, A. Ingram, S. Kozyukhin, O. Shpotyuk, Free volume fragmentation in glassy chalcogenides during natural physical ageing as probed by PAL spectroscopy, *J. Non-Cryst. Solids* 377 (2013) 49–53.
- [27] B. Bergersen, M.J. Stott, The effect of vacancy formation on the temperature dependence of the positron lifetime, *Solid State Commun.* 7 (1969) 1203–1205.
- [28] K. Krause-Rehberg, H.S. Leipner, Determination of absolute vacancy concentrations in semiconductors by means of positron annihilation, *Appl. Phys. A-Mater.* 64 (1997) 457–466.
- [29] J. Gebauer, F. Rudolf, A. Polity, R. Krause-Rehberg, J. Martin, P. Becker, On the sensitivity limit of positron annihilation: detection of vacancies in as-grown silicon, *Appl. Phys. A-Mater.* 68 (1999) 411–416.
- [30] P.M.G. Nambissan, C. Upadhyay, H.C. Verma, Positron lifetime spectroscopic studies of nanocrystalline  $\text{ZnFe}_2\text{O}_4$ , *J. Appl. Phys.* 93 (2003) 6320–6326.
- [31] P. Masselin, D. Le Coq, L. Calvez, E. Petracovschi, E. Lépine, E. Bychkov, X. Zhang, CsCl effect on the optical properties of the  $80\text{GeS}_2\text{-}20\text{Ga}_2\text{S}_3$  base glass, *Appl. Phys. A-Mater.* 106 (2012) 697–702.
- [32] H. Klym, A. Ingram, O. Shpotyuk, R. Szatanik, Free-volume study in  $\text{GeS}_2\text{-Ga}_2\text{S}_3\text{-CsCl}$  chalcogenide glasses using positron annihilation technique, *Phys. Procedia* 76 (2015) 145–148.
- [33] H. Klym, A. Ingram, O. Shpotyuk, O. Hotra, A.I. Popov, Positron trapping defects in free-volume investigation of Ge-Ga-S-CsCl glasses, *Radiat. Meas.* 90 (2016) 117–121.